The InSAR Feasibility Tool

Moretto S.[a,b], Paolo M. [a,b], Lefort T.[c], Partington K.[c], Bozzano F. [a,b]

[a] *NHAZCA S.r.l., Spin-off di Università degli Studi di Roma "La Sapienza", Via Bachelet n.12, 00185, Roma*

[b] *Dipartimento di Scienze della Terra., Università degli Studi di Roma "La Sapienza", P.le Aldo Moro n.5, 00185, Roma*

[c] *Geocento Limited., Atlas Building, Fermi Avenue, Harwell, Didcot, Oxfordshire OX11 0QX UK.*

1. Introduction

Satellite InSAR (Synthetic Aperture Radar Interferometry) is an active remote sensing technique for ground deformation monitoring. A-DInSAR (Advanced Differential InSAR) processing techniques in particular can be used to obtain time series of displacement of both the ground and structures (such as: outcropping rocks, buildings, slopes, etc.) reaching millimetre accuracy (Ferretti et al. 2000, 2001; Kampes et al. 2006). The approach is based on multi-image analysis that supports estimation and removal of atmospheric noise. The basic requirement for the application of A-DInSAR techniques is the availability of a good number of multi-temporal SAR images acquired over the same area.

The availability of SAR images is determined by the acquisition plans of different satellite missions that have operated since the early 1990s. Over the last few years, an increase in the number of satellite missions has provided an opportunity to perform A-DInSAR studies at a global level. However, at the same time, the search for imagery in the archives of the different operators has become more complex and time consuming. In order to address this challenge, NHAZCA S.r.l. and Geocento Ltd have jointly developed the InSAR Feasibility Tool, a web based platform capable of quickly assessing the availability of satellite images suitable for A-DInSAR analysis (i.e. interferometric stacks). The users can use the tool to assess the feasibility of A-DInSAR analysis according to the availability of satellite SAR data.

2. Satellite InSAR Overview

A-DInSAR is a powerful technique able to measure and monitor surface displacements of the ground and structures over time, reaching millimetric accuracy, for those measurement points characterized by high intensity and stability of the backscattered signal (Ferretti et al. 2000, 2001, 2011; Berardino et al. 2002; Kampes et al. 2006). A-DInSAR is a multi-image processing approach suitable for both wide areas (thousands of square kilometres) and small areas (i.e. single slope or structure), with the capability of providing time series of displacements of the observed targets. A-DInSAR is based on the Differential InSAR technique (DInSAR). This technique exploits the information contained in the phase of the

signal of two complex SAR images acquired in different times over the same area, used to form the so-called interferogram (Crosetto et al. 2016). The interferogram is computed by cross-multiplying the first SAR image with the complex conjugate of the second (Ferretti et al. 2007). The resulting interferometric phase (φ_{int}) is the phase difference between the two images, with the following contributing phase elements:

$$\varphi_{int} = \varphi_{topo} + \varphi_{flat} + \varphi_{disp} + \varphi_{atmo} + \varphi_{err} \quad (1)$$

where φ_{topo} represents the contribution related to the topography, φ_{flat} represents the flat Earth phase component due to different look angles of the two acquisitions, φ_{disp} is the contribution related to displacement, φ_{atmo} is the phase related to different athmospheric conditions and φ_{err} represents the error related to uncontrolled effects (e.g. decorrelation, position along the satellite orbit, etc.).

The differential interferogram is formed by subtracting the φ_{topo} and φ_{flat} contributions from the interferometric phase, by using a reference DEM (Digital Elevation Model) and a reference ellipsoid respectively, thus allowing retrieval of the phase component related to displacement. Figure 1 shows an example of a Sentinel-1 (European Space Agiency) differential interferogram, related to the co-seismic interval of the Norcia earthquake (30th October 2016, Norcia, Central Italy).

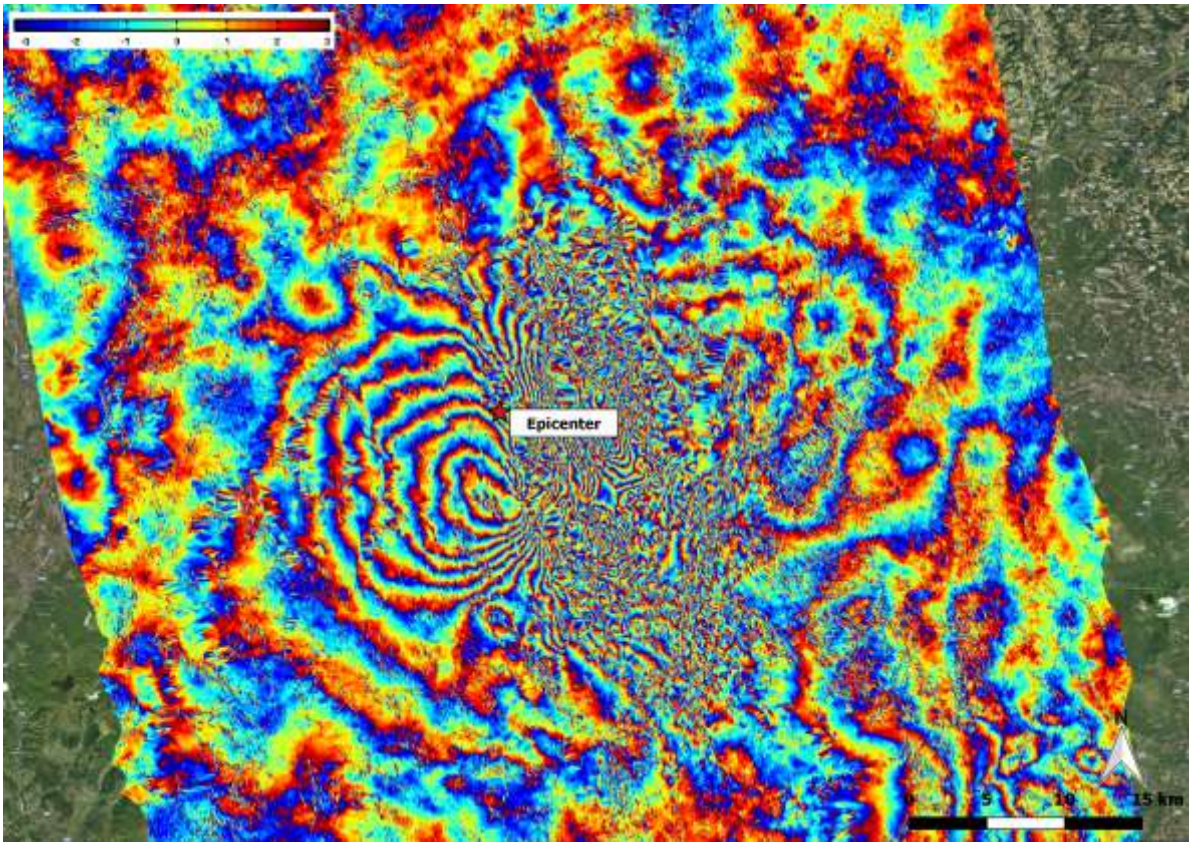

Figure 1. Sentinel-1 interferogram of the co-seismic interval related to the Norcia earthquake (30th October 2016, Mw 6.5, 42.84°N 13.11°E, 07:40 local time).

To generate the interferogram shown in Figure 1, two SAR images were acquired on 27/10/2016 and 02/11/2016 from an ascending orbit pass (i.e. passing from South to North looking in the right direction). The deformation produced by the earthquake is highlighted by the presence of the so-called "interferometric fringes". The colour cycle of one fringe (from red to blue) corresponds to a displacement of half of the wavelength. Thus, considering the characteristics of the Sentinel-1 satellites, one fringe corresponds to a displacement of 2.8 cm in the Line Of Sight (LOS) direction.

DInSAR does not allow the estimation of φ_{atmo} component, but this can be removed by means of the A-DInSAR technique. A-DInSAR methods exploit multiple SAR images acquired over the same area, isolating φ_{disp} from the other phase components using suitable data processing algorithms (Crosetto et al. 2016).

The main products of an A-DInSAR analysis are (a) the time series of displacement and (b) the average velocity, that can be estimated over the measurement points characterised by a persistent (PSs - Persistent Scatterers) or distributed (DSs – Distributed Scatterers) backscatter behaviour (Ferretti et al. 2000,2001,2011; Perissin & Wang 2012) (Figure 2). It is worth mentioning that the displacements are measured along the LOS, i.e. the path direction between the sensor and target. In Figure 2 an example of A-DInSAR result is reported. The analysis was carried out by processing 46 COSMO-SkyMed images acquired over the time period between 2011 and 2015. The images were acquired in the Stripmap mode, characterised by a resolution of 3x3 meters in slant-range and azimuth. In Figure 2, the settlement processes that were affecting the road (red points) are clearly observable, characterized by an average velocity trend of about 10 mm/year.

Its capabilities and peculiarities make the InSAR technique a suitable and powerful tool for several applications such as monitoring of subsidence processes (e.g. due to oil and gas extraction or water extraction), slope stability assessment, structure/infrastructure monitoring (i.e. dams, buildings, highway, viaducts, etc.), tunnelling-induced ground deformation monitoring, land use planning and monitoring of volcanic and seismic activity.

In order to retrieve the time series of displacement, a minimum number of 15–20 images collected with the same acquisition geometry is required (Crosetto et al 2016). Furthermore, the larger the number of available scenes the better the quality of the average velocity estimation and time series of displacement. A collection of images that can be processed together using A-DInSAR methods is called an interferometric stack.

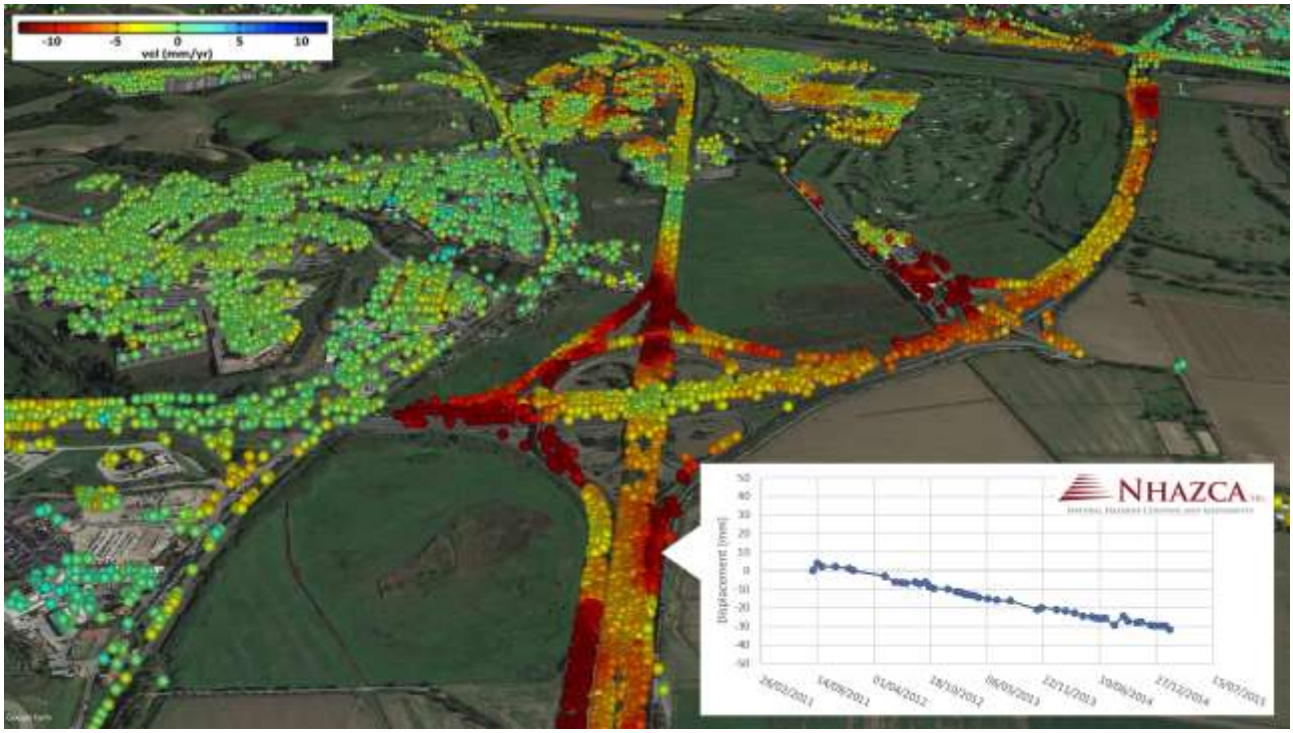

Figure 2. Example of A-DInSAR results from COSMO-SkyMed images. Each measurement point is a PS and its colour indicates the magnitude and the direction of the average velocity (in mm/year) along the LOS. Yellow to red colours indicate movements away from the sensor, while light blue-blue colours indicate movements toward the sensor. Green points are considered as stable.

3. Availability of SAR imagery and Satellite Missions

The presence of SAR data is constrained by the data acquisition plans and tasking priorities of SAR satellite missions, including those of relevant space agencies . Several space agencies have supported and continue to support different SAR missions (https://www.unavco.org) such as:

- European Space Agency (ESA) with ERS-1, ERS-2, Envisat and Sentinel-1 satellites;
- Japan Aerospace Exploration Agency (JAXA) with JERS-1, ALOS-1 and ALOS-2;
- Canadian Space Agency (CSA) through Radarsat-1, Radarsat-2 and the future Radarsat constellation;
- Deutsches Zentrum für Luft- und Raumfahrt e.V. (DLR) by means of TerraSAR-X and TanDEM-X;
- Indian Space Research Organization (ISRO) with RISAT-1 and NISAR (w/ NASA);
- Comision Nacional de Actividades Espaciales with SAOCOM;
- Italian Space Agency (ASI) with the COSMO-SkyMed Constellation;
- Instituto National de Técnica Aeroespacial (INTA) with PAZ;
- Korea Aerospace Research Institute (KARI) with KOMPSat-5.

SAR images have been available since 1992, when the first global systematic acquisition of SAR scenes was initiated by the European Space Agency using the ERS-1 satellite which was launched in July 1991. Since then, several satellites have been placed in orbit and today there are several active SAR missions: i) COSMO-SkyMed constellation composed by 4 satellites (X-band); ii) TerraSAR-X and TanDEM-X (X-band); iii) Sentinel-1 constellation composed by 2 satellites (C-band); iv) Radarsat-2 (C-band); v) ALOS-PALSAR-2 (L-band),; vi) PAZ (X-band); vii) KOMPSat-5 (X-band); viii) SAOCOM (L-band) and ix) RISAT-1 (C-band).

In Table 1 the principal SAR satellite missions and their features are summarised, while Figure 3 shows the past, current and future temporal distribution of satellite missions.

Satellite sensors have very different characters in terms of: i) operational period; ii) revisit time (i.e., the time elapsed between consecutive interferometric acquisitions generated by sensors with identical features); iii) sensor wavelength (λ), v) spatial resolution and vi) incidence angle (geometry of ground observation). This variety of configurations is important to note as many factors influence A-DInSAR results. Indeed, the technical characteristics of both the SAR sensors and interferometric stack features can play a key role in the potential value of A-DInSAR results. For example (Rocca 2013):

i) the number of images, the time period covered and the temporal resolution (revisit time) of the dataset may affect the quality of the results (e.g. few images distributed in a long time period may not allow to reach satisfactory results);
ii) geometrical aspects of the acquisition influence the capability of monitoring specific areas (e.g. ascending orbit acquisition geometries are more suitable for monitoring east-facing slopes than descending ones, because of the geometrical distortions affecting the SAR scenes);
iii) the sensor wavelength influences many aspects of the results, not least the capability to measure certain deformation trends and to penetrate vegetation;
iv) the spatial resolution affects the spatial density of measurement points.

Despite the large number of SAR satellite sensors, the data acquisition policy of these missions (e.g. the regular acquisition over given areas vs. on-demand acquisitions) greatly influences the availability of SAR data, which can be very irregular both in time and space (Crosetto et al. 2016). For this reason, the first step of an interferometric study is to assess the availability of SAR satellite images in terms of interferometric stacks.

Table 1. Selection of the principal SAR satellite interferometric systems and their characteristics (from Zhou et al. 2009 modified).

Sensor	Country	Operational Period	Revisit Time (days)	λ (cm)	Acquisition	Resolution (m) (azimuth x range)	Look angle
X Band							
COSMO-SkyMed	Italy	2007÷	16/8/4	3.125	*SL	1	25°-50°
					*SM	3 x 3	25°-50°
					*SC	30 x 100	25°-50°
TerraSAR-X	Germany	2007÷	11	3.1	*SL	2 x (1.5-3.5)	20°-55°
					*HR SL	1 x (1.5-3.5)	20°-55°
					*SM	3 x (3-6)	20°-45°
					*SC	16 x 16	20°-45°
PAZ	Spain	2012÷	11	3.1	*SM	3x3	15°-60°
					*SC	16x6	15°-60°
					*SL	1x1	15°-60°
					HR Spotlight	<1x1	15°-60°
KOMPSat-5	Korea	2013 ÷	28	3.2	*SL	1x1	20°-45°
					*SM	3x3	20°-45°
					*SC	20x20	20°-45°
C Band							
ERS-1/2	Europe	1992÷2001	35	5.66	ASAR	6 x 25	20°-26°
Envisat	Europe	2003÷2010	35	5.63	Image	6 x 24	15°-45°
RADARSAT-1	Canada	1995÷2013	24	5.55	Fine	9 x (8,9)	37°-47°
					Standard	28 x (21-27)	20°-49°
					Wide	28 x (23,27,35)	20°-45°
					*SC narrow	50 x 50	20°-49°
					*SC wide	100 x 100	20°-49°
RADARSAT-2	Canada	2007 ÷	24	5.55	Ultra-fine	3 x 3	30°-49°
					Fine	8 x 8	30°-50°
					Standard	26 x 25	20°-49°
					Wide	26 x 30	20°-45°
					*SC narrow	50 x 50	20°-46°
					*SC wide	100 x 100	20°-49°
Sentinel-1	Europe	2014÷	6	5.6	*WS	20 x 5	29°- 46°
					*SM	5 x 5	29°- 46°
L Band							
JERS-1	Japan	1995	44	23.5		18 x 18	35°
ALOS/PALSAR	Japan	2006÷2011	46	23.62	Fine 1	10 x (7-44)	8°-60°
					Fine 2	10 x (14-88)	8°-60°
					*PL	10 x (24-89)	8°-30
					*SC	100 x 100	18° -43°
ALOS-PALSAR-2	Japan	2014÷	14	23.6	*SM	3x3	8°-70°

*SC – ScanSAR; SL – Spotlight; SM – Stripmap; WS - wide swath; HR – high resolution;

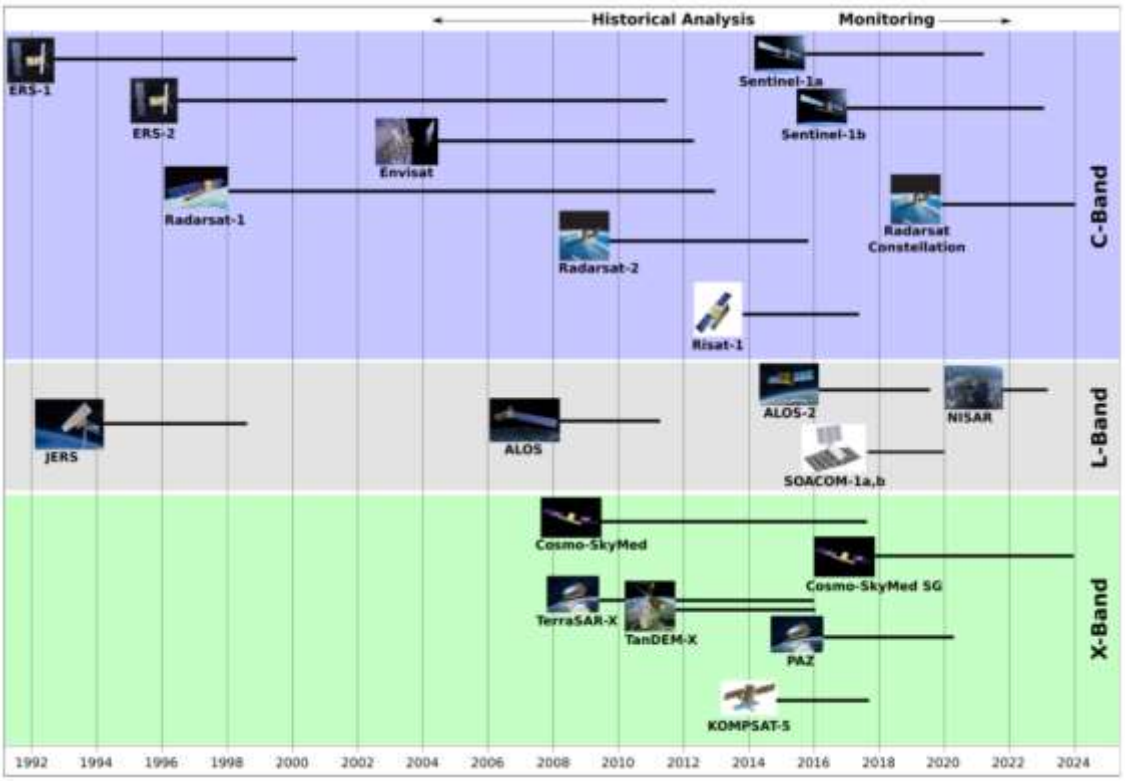

Figure 3. Temporal distribution of the principal SAR satellite missions (from https://www.unavco.org)

4. InSAR Feasibility Tool

The main objective of the InSAR Feasibility Tool is the identification of suitable SAR images that can be used for A-DInSAR applications.

As mentioned above, in order to perform an A-DInSAR analysis, the images have to satisfy some criteria. Indeed, only imagery belonging to a so-called interferometric stack can be processed in order to retrieve ground deformation.

A necessary condition for a data-stack formation is to use only SAR images acquired with the same sensor, geometry (ascending or descending) and features (i.e., same acquisition mode, same look angle, same resolution, same polarization, etc.). The InSAR Feasibility Tool takes these image selection constraints into account, thus identifying the interferometric stacks.

The InSAR Feasibility Tool (Figure 4), developed by NHAZCA S.r.l. (www.nhazca.com) and Geocento L.t.d. (www.geocento.com), is an open access web-based platform available online at: www.sarinterferometry.com.

The user has the ability to set the Area of Interest (AoI) and the period of interest, which are then used to quickly determine the availability of interferometric stacks for that area and time period. This is done by sending the query through an Application Programming Interface (API) to check metadata associated with relevant SAR satellite missions, which Geocento collects routinely from multiple suppliers to support its image search and discovery platform, EarthImages. Each SAR image that covers the time and area of interest

is checked against existing image stacks to determine whether it matches and thus can augment the interferometric stack. If no stack exists, then the image may form the first member of a new interferometric stack. The outcomes of the search, listed in the results table (left in Figure 4), are represented by the available stacks ("options") belonging to different satellite missions. The number of images that composed each stack is reported in parenthesis. By pressing the "i" button, additional information about each stack can be observed (e.g. the name of the satellite, the time acquisition line, etc.). At present, the Tool supports the following satellite missions: TerraSAR-X and TanDEM-X, Radarsat-1 and Radarsat-2 and Sentinel-1, and it will include other past, present and future SAR satellites in the next release.

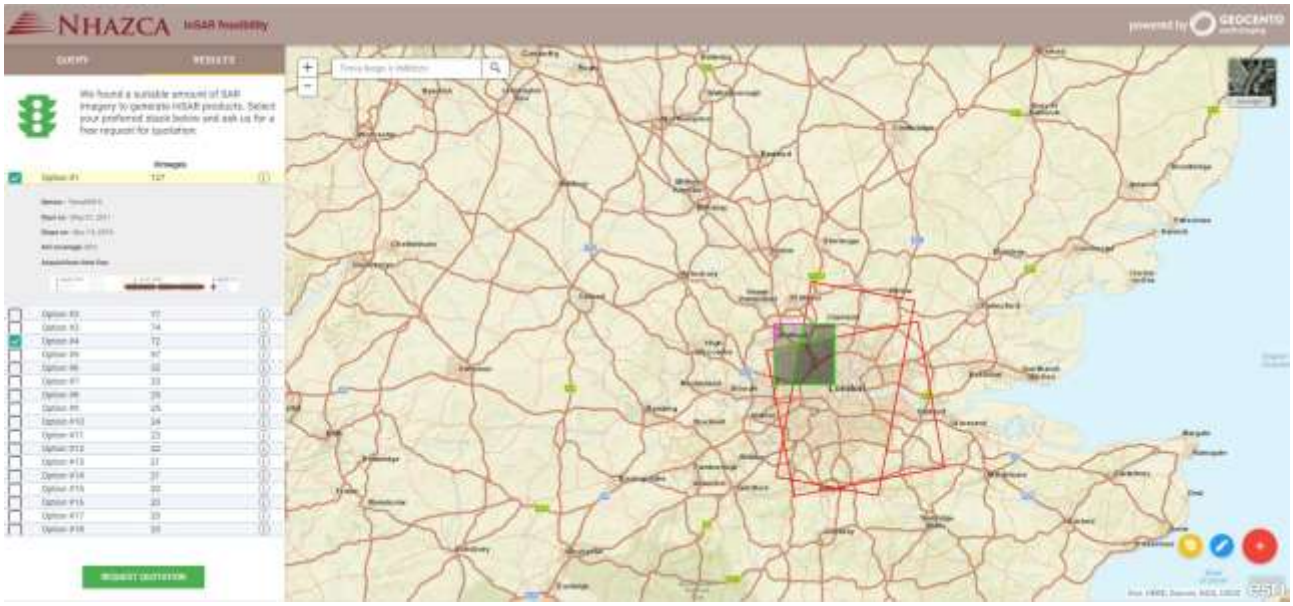

Figure 4. Nhazca and Geocento InSAR Feasibility Tool (http://projects.geocento.com/nhazca/).

5. Conclusions

The growing number of satellite missions and images can make the search of SAR data complex. Furthermore, the search of suitable SAR images can be difficult, time consuming and unreasonably complex for a non-expert user. The InSAR Feasibility Tool has been developed in order to assist the users in evaluating the availability of suitable SAR data for an A-DInSAR analysis. The open access application can be found at www.sarinterferometry.com. After a simple registration process, users can use the tool to carry out quick assessments of the feasibility of A-DInSAR for their own areas of interest.

References

Berardino P., Fornaro G., Lanari R., & Sansosti E. 2002. A new algorithm for surface deformation monitoring based on small baseline differential SAR interferograms. IEEE Trans. Geosci. Remote Sensing. 40, 2375 – 2383.

Crosetto M., Monserrat O., Cuevas-González M., Devanthéry N., Crippa B. 2016. Persistent Scatterer Interferometry: A review. ISPRS Journal of Photogrammetry and Remote Sensing 115, 78–89

Crosetto M., Crippa B., Biescas E., 2005. Early detection and in-depth analysis of deformation phenomena by radar interferometry. Eng. Geol. 79, 81–91.

Ferretti A., Fumagalli A., Novali F., Prati C., Rocca F., Rucci A. 2011. A new algorithm for processing interferometric data-stacks: SqueeSAR. IEEE Transactions on Geoscience and Remote Sensing 49 (9), 3460-3470.

Ferretti A., Monti-Guarnieri A., Prati C., Rocca F., & Massonnet D. 2007. InSAR Principles-Guidelines for SAR Interferometry Processing and Interpretation. (K. Fletcher, Ed.) (ESA Public.). Noordwijk, The Netherlands: ESA Publications. Retrieved from http://adsabs.harvard.edu/abs/2007ESATM

Ferretti A., Prati C. &. Rocca F.; 2001. Permanent scatterers in SAR interferometry. IEEE Trans. Geosc. and Remote Sens. 39(1), 8-20.

Ferretti A., Prati C., & Rocca F.; 2000. Nonlinear subsidence rate estimation using permanent scatterers in differential SAR interferometry. IEEE Transactions on Geoscience and Remote Sensing, 38(5), 2202–2212. doi:10.1109/36.868878.

Hanssen R.F., 2005. Satellite radar interferometry for deformation monitoring: a priori assessment of feasibility and accuracy. International Journal of Applied Earth Observation and Geoinformation, 6(3), 253-260.

Kampes B. M. 2006. Radar Interferometry Persistent Scatterers Technique. (Springer, Ed.). Dordrecht, The Netherlands.

Perissin D. & Wang T., 2012. Repeat-Pass SAR Interferometry With Partially Coherent Targets. IEEE Trans. on Geosc. and Remote Sens. 501, 271, 280.

Rocca A. 2013. Ground deformation analysis by means of satellite SAR interferometry: spatial and temporal charachterization and forecasting potential. PhD Thesis in Earth Sciences, Department of Earth Sciences . Sapienza University of Rome.

Zhou X., Chang N.B and Li S. 2009. Applications of SAR Interferometry in Earth and Environmental Science Research. Sensors, 9, 1876-1912; doi:10.3390/s90301876

Link

www.nhazca.com

www.geocento.com

www.sarinterferometry.com

http://projects.geocento.com/nhazca/

https://www.unavco.org

https://www.unavco.org/instrumentation/geophysical/imaging/sar-satellites/sar-satellites.html